

Refractory Two-Dimensional Titanium Nitride Structures with Extremely Narrow Surface Lattice Resonances at Telecommunication Wavelengths

Vadim I. Zakomirnyi,^{1,2} Iliia L. Rasskazov,^{3, a)} Valeriy S. Gerasimov,¹ Alexander E. Ershov,^{1,4,5} Sergey P. Polyutov,¹ and Sergei V. Karpov^{1,5,6}

¹⁾*Institute of Nanotechnology, Spectroscopy and Quantum Chemistry, Siberian Federal University, Krasnoyarsk 660041, Russia*

²⁾*Division of Theoretical Chemistry and Biology, School of Biotechnology, KTH Royal Institute of Technology, 10691 Stockholm, Sweden*

³⁾*Beckman Institute for Advanced Science and Technology, University of Illinois at Urbana-Champaign, Urbana, IL 61801, USA*

⁴⁾*Institute of Computational Modeling, Federal Research Center KSC SB RAS, 660036, Krasnoyarsk, Russia*

⁵⁾*Siberian State University of Science and Technology, Krasnoyarsk 660014, Russia*

⁶⁾*L. V. Kirensky Institute of Physics, Federal Research Center KSC SB RAS, 660036, Krasnoyarsk, Russia*

(Dated: 6 September 2017)

Regular arrays of plasmonic nanoparticles have brought significant attention over the last decade due to their ability to support localized surface plasmons (LSPs) and exhibit diffractive grating behavior simultaneously. For a specific set of parameters, i.e. period, particle shape, size, and material; it is possible to generate super-narrow surface lattice resonances (SLRs) that are caused by interference of the LSP and the grating Rayleigh anomaly. In this Letter, we propose plasmonic structures based on regular 2D arrays of TiN nanodisks to generate high- Q SLRs at important telecommunication range, which is quite difficult to achieve with conventional plasmonic materials. Position of SLR peak can be tailored within the whole telecommunication bandwidth (from $\approx 1.26 \mu\text{m}$ to $\approx 1.62 \mu\text{m}$) by varying the lattice period, while Q -factor is controlled by changing nanodisks sizes. We show that Q -factor of SLRs can reach a value of 2×10^3 , which is the highest reported Q -factor for SLRs at telecommunication wavelengths so far. Tunability of optical properties, refractory behavior and low-cost fabrication of TiN nanoparticles paves the way for manufacturing cheap nanostructures with extremely stable and adjustable electromagnetic response at telecommunication wavelengths for a large number of applications.

PACS numbers: 42.70.-a, 73.20.Mf, 78.67.-n, 81.05.Je

Regular arrays of plasmonic nanoparticles exhibit a unique feature: the existence of collective modes that originate from strong coupling between localized surface plasmons (LSPs) and the grating Rayleigh anomalies. Such strong hybrid coupling gives rise to narrow surface lattice resonances (SLRs) which tremendously outperform quality factor Q of LSP. SLRs have attracted significant attention during the last decade starting from pioneering theoretical¹⁻³ and experimental⁴⁻⁶ studies with extension to promising applications in vibrational spectroscopy⁷, ultranarrow band absorption⁸, sensing^{9,10}, lasers¹¹ and fluorescence enhancement^{12,13}. SLRs were studied in a wide variety of periodic nanostructures with different kinds of unit cells: single¹⁴ or double-stack¹⁵ nanodisks, core-shell cylinders¹⁶, nanoparticle dimers^{17,18}, nanorings¹⁹, split-ring resonators²⁰, oligomers²¹ and more complex configurations²²⁻²⁵.

Nowadays, most of attention is fixed on gratings made of classic plasmonic materials (Au and Ag) with LSP peak of individual particles lying in the visible or near-infrared (NIR) regions. The position of SLR peak in

such structures is strictly limited to visible and NIR since the strongest coupling between LSP and Rayleigh anomaly takes place at certain wavelength^{1,2,14}. SLR peak is red shifted compared to the LSP peak and slightly blue-shifted compared to position of Rayleigh anomaly. Telecommunication wavelength range, which is important for large number of applications and especially for hybrid nanophotonics interconnects²⁶, remains almost unreachable for SLRs with conventional plasmonic materials. Utilization of non-spherical or non-homogeneous particles may lead to significant shift of LSP to longer wavelengths, however, it is quite complicated to cover telecommunication bandwidth with classic plasmonic materials keeping reliable values of the SLR Q -factor. Although regular Au nanostructures on metal-dielectric substrates possess SLRs at telecommunication wavelengths with high quality factors^{27,28} (up to $Q \approx 300$), such performance is notably poorer than the one recently reported for SLRs in the visible range for 2D arrays of Au nanodisks¹⁴ with $Q > 1000$.

Here we propose to enhance SLRs within the telecommunication wavelength range by utilizing so-called alternative plasmonic materials²⁹. Among numerous possible choices, titanium nitride (TiN) has been considered as the most promising candidate to reduce the supremacy

^{a)}Electronic mail: iliar@illinois.edu

of gold and silver^{30–32} in a number of applications^{33–35}. Low-cost large-area fabrication of TiN nanostructures³⁶, full CMOS-compatibility³⁷, refractory behavior^{38,39} and wide tunability of optical and structural properties^{30,40} make TiN an attractive alternative plasmonic material. However, what is really important, the LSP peak of a single TiN nanoparticle lies in the NIR region³⁰, which is crucial for tailoring the position of SLR peak beyond the visible range. The last feature represents the cornerstone of this work in which we provide the concept of 2D regular structures from TiN nanodisks with high- Q factor SLRs at telecom wavelengths.

It is well known fact that optical properties of TiN as a non-stoichiometric material strongly depend on its synthesis conditions. TiN thin films exhibit color variations⁴¹ and even notable metallic luster³⁰ with changing composition and lattice parameters which can be controlled, for example, by varying temperature of its deposition. Thus, for a particular set of deposition parameters, it is possible to enhance plasmonic behavior of TiN structures⁴⁰. Therefore, to provide a comparative analysis of SLRs performance, we have chosen two different datasets for TiN dielectric permittivity ϵ : (i) recently acquired temperature- and size-dependent data for plasmonic-like TiN *thin films* from Ref.⁴² and (ii) widely used tabulated data for *bulk* TiN at room temperature from Ref.⁴³. **This choice of datasets will naturally reveal the qualitative influence of TiN deposition parameters on SLRs performance.**

Before discussing SLRs on regular arrays, it is insightful to investigate plasmonic properties of a single TiN nanoparticle. Although it is obvious that the shape of a nanoparticle is an important factor which definitely affects Q -factor of SLR, we restrict ourselves to nanodisks. A nanodisk is a quite easy-to-fabricate shape from an experimental point of view, and one of the most reliable shapes for high- Q SLRs¹⁴. We consider nanodisks with three different diameters d : 160, 180 and 200 nm, and fix height to $h = d/2$ for all cases. Normal plane wave incidence with polarization of electric field perpendicular to the symmetry axis of a nanodisk was used in simulations, as shown in Fig. 1(c). Extinction cross section σ_{ext} of a nanodisk was calculated with commercial Lumerical finite-difference time-domain (FDTD) software package⁴⁴. **Data for ϵ in Ref.⁴² are provided for thin films with different thicknesses, so we have implemented linear interpolation to assess ϵ for each particular size of nanodisks.**

Figures 1(a–b) clearly show that the LSP peak of a single nanodisk lies from $\lambda \approx 950$ nm to $\lambda \approx 1050$ nm, depending on its size. It is quite difficult to tailor the LSP peak to this wavelength region and to maintain its quality factor with homogeneous nanoparticles made of conventional plasmonic materials. Comparison of σ_{ext} calculated with two different datasets for ϵ shows that tunability of TiN optical properties makes it possible to increase noticeably LSP quality factor of a single nanodisk, which is preferable for enhancing LSP-Rayleigh

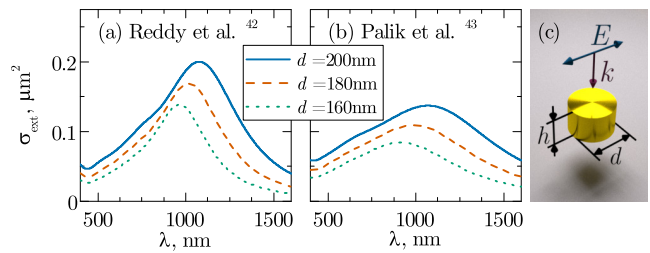


FIG. 1. (a–b) Extinction spectra of a single TiN nanodisk with a given diameter d and height $h = d/2$. Nanodisk is embedded in homogeneous medium with $n_m = 1.5$. Spectra are provided for two different datasets for ϵ of TiN: Ref.⁴² and Ref.⁴³; (c) Schematic representation of a single TiN nanodisk illumination.

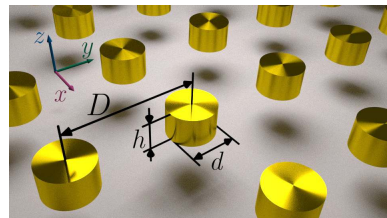


FIG. 2. The sketch of a system under consideration: 2D regular lattice with period D comprised of TiN nanodisks with height h and diameter d .

anomaly hybridization.

Then, we continue with the spectral properties of 2D regular arrays of TiN nanodisks, which schematic representation is depicted in Fig. 2. The period D of the lattice is varied to match the $(\pm 1, 0)$ and $(0, \pm 1)$ Rayleigh anomalies⁴⁵, which positions for the case of normal incidence and homogeneous surrounding with refractive index n_m are defined as $\lambda_{p,q} = n_m D (p^2 + q^2)^{-1/2}$, where p and q are integers corresponding to diffraction order. We assume that nanoparticles are embedded in a homogeneous medium with $n_m = 1.5$. This kind of structures can be fabricated by deposition of TiN nanoparticles onto glass substrate and subsequently covering them with poly(methyl methacrylate) superstrate. The same approach was used to obtain Au and Al nanodisks arrays in homogeneous environment¹⁴. Symmetric surrounding is the key ingredient in this model, because quality factor of a SLR sharply drops in the case of half-space geometry comprising substrate and superstrate with non-matching refractive indices^{14,46,47}.

FDTD method is a comprehensive and well-established approach for solution of electromagnetic problems which shows excellent agreement with experimental results for SLRs in various types of nanostructures^{6,8,9,11,14,15,23,27,48}. However, high- Q resonances with significant spatial extent (which is the case for SLRs⁴⁹) require careful implementation of FDTD approach. Thus, special attention should be paid to the simulation setup. We apply periodic boundary condi-

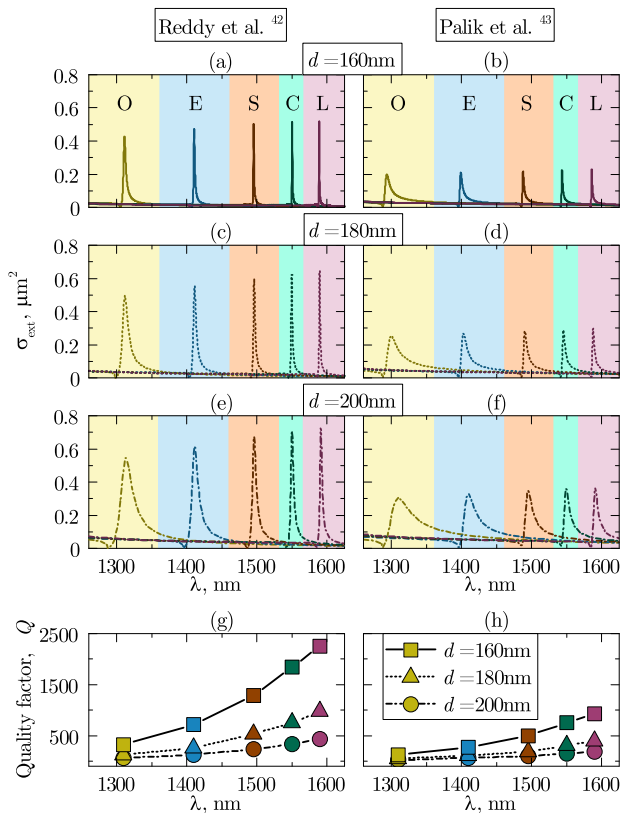


FIG. 3. (a–f) Extinction spectra (per particle) for 2D regular arrays from TiN nanodisks with various diameter d and height $h = d/2$. Five different lattice periods D were chosen to generate SLRs at each telecommunication band: $D_O = 857$ nm, $D_E = 929$ nm, $D_S = 989$ nm, $D_C = 1026$ nm, $D_L = 1055$ nm; (g–h) Quality factors Q for corresponding peaks at: $\lambda_O = 1310$ nm, $\lambda_E = 1410$ nm, $\lambda_S = 1495$ nm, $\lambda_C = 1550$ nm, $\lambda_L = 1590$ nm. Two different datasets for ϵ of TiN are used in calculations: Ref.⁴² (left panel) and Ref.⁴³ (right panel).

tions at the lateral boundaries of a unit cell (single nanodisk), while perfectly matched layer (PML) boundary conditions were used on the remaining top and bottom sides. To avoid undesired reflections on the PMLs and overestimation of the SLR width, we have performed extensive convergence tests for each set of parameters to assure the adequacy of calculations reported in this Letter. These tests show that sufficiently large simulation boxes (up to 32 – 40 μm along z -axis) are required for convergence of FDTD method. In all cases, nanostructures are illuminated from the top by plane waves with normal incidence along z axis and polarization along x or y axis. We calculate transmission T at the bottom of the structure and then characterize its spectral properties by $\sigma_{\text{ext}} = D^2(1 - T)$ in accordance with Refs^{4,14,50}. An adaptive mesh was used for an accurate description of the nanodisk shape.

Figures 3(a–f) show that SLRs are easily tailored through the whole telecommunication wavelength range

by varying lattice period D . It is highly important to choose appropriate size of nanodisks: for fixed D , SLR becomes extremely narrow for $d = 160$ nm. For example, the SLR width at L-band can be dramatically reduced to ≈ 1 nm, as shown in Fig. 3(a). Although it is clear that further decrease of nanodisks sizes leads to increase of Q -factor, we limit the discussion with $d = 160$ nm value, because of extremely slow convergence of FDTD method for such narrow-band resonances. In real experiment, Q would likely increase for $d < 160$ nm with fixed D , however, at the same time, the position of SLR peak may significantly depend on any imperfections: disorder of nanodisks positions or sizes. Thus, controlled generation of SLRs with higher Q -factor becomes a complicated task. It can be also seen from Figs 3(g–h) that for fixed nanodisks sizes, the quality factor Q gradually increases for larger values of D which is consistent with results from Ref.¹⁴ for the visible range. For the most important telecommunication C-band, at $\lambda = 1550$ nm, quality factor of SLR is up to $Q \approx 1850$, which breaks the actual record of $Q \approx 300$ for SLRs at the same wavelength²⁷. It is also notable that quality factors of SLRs calculated with ϵ from Ref.⁴² are about twice as much as ones calculated for data from Ref.⁴³. Such a considerable difference in SLRs Q -factor is expected, because bulk permittivity significantly differs from ϵ of thin films. However, Figures 3(g–h) reveal the crucial importance of size-dependence of TiN optical properties which is controlled by varying deposition parameters. The lateral fact is frequently overlooked in comparative analysis of conventional plasmonic materials and metal nitrides³¹, where the ϵ for a *bulk* TiN is usually used in simulations. Therefore, in real applications, appropriate tuning of TiN optical properties by varying its deposition parameters can considerably enhance its plasmonic behavior which is necessary for narrow high- Q SLRs.

Finally, TiN, as a refractory plasmonic material, exhibit extraordinary stability at high temperatures³⁸ compared to conventional Au⁵¹. Suppression of LSP resonance under aggressive conditions may totally deteriorate LSP-lattice hybridization, therefore the refractory behavior of TiN may become an additional advantage in the case of SLR generation at high temperatures. Experimental measurements of TiN dielectric permittivity in Ref.⁴² imply that lattice dynamics, electron-phonon scattering and other temperature-dependent phenomena are already included in $\epsilon(T)$. Therefore, FDTD simulations remain consistent, and additional consideration of these effects is not required. Figure 4 provides temperature-dependent SLRs behavior at the most important telecommunication wavelength $\lambda = 1550$ nm. It can be seen, that SLR resonance is suppressed at high temperature T , and the SLR peak position shifts by no more than $\Delta\lambda \approx 0.3$ nm at $T = 900^\circ\text{C}$ compared to SLR peak at room temperature. Thus, the quality factor Q drops roughly 2 times keeping the position of SLR almost the same, which is significantly better than for conventional plasmonic materials, whose LSPs are almost sup-

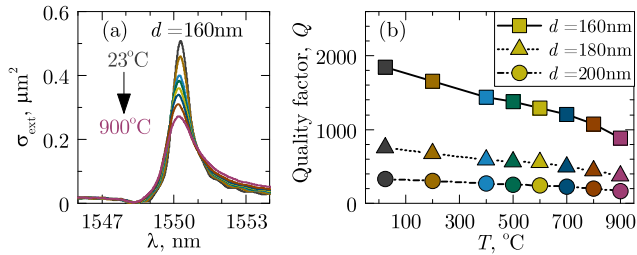


FIG. 4. (a) Temperature-dependent extinction spectra (per particle) and (b) corresponding quality factors Q for SLRs in 2D lattices of TiN nanodisks with fixed $D = 1026$ nm and for different diameter d and height $h = d/2$. Temperature-dependent values of ε from Ref.⁴² were used in simulations.

pressed⁵² at high temperatures.

Several possible issues related to experimental verification of obtained results are worth discussion. First, it is more possible to synthesize TiN nanopillars³⁷ in real experiment rather than nanodisks. However, it is easy to keep or even outperform reported values of Q by varying properly nanoparticles shapes and sizes. Second, it is quite difficult to perfectly match substrate's and superstrate's refractive indices, which for sure might significantly suppress SLRs. However, these complications are easily surpassed by generating parallel SLRs⁴⁸ or mimicking dipole resonances by excitation of monopoles above a mirror plane⁵³. Both of these approaches exhibit greater tolerance to anti-symmetry of the surrounding medium refractive index. Finally, TiN dielectric permittivity ε in real experiment may significantly differ from datasets considered in this Letter. Nevertheless, reported results show that even TiN nanodisks with low- Q LSP (for ε taken from Ref.⁴³) exhibit high- Q SLRs (up to $Q = 1000$) for particular set of geometric parameters. Thus, high- Q SLRs in real experiment can be achieved by careful choice of TiN deposition parameters and tuning its optical behavior for each particular case.

To conclude, we have shown that regular 2D arrays of TiN nanodisks are promising hybrid plasmonic systems which possess super-narrow high- Q SLRs within the whole telecommunication bandwidth. Quality factor and position of SLR peak can be tailored through varying the lattice period D and sizes of nanoparticles. Refractory properties and large tunability of TiN optical properties make this material an attractive alternative to conventional Au and Ag which fail to tailor high- Q SLRs to telecom. Further development and extension of reported approach open an opportunity to go beyond the telecommunication range and to increase the performance of SLRs in the IR region which might be promising in mid-IR⁵⁴ and vibrational⁷ spectroscopies.

The authors thank Vadim Markel for careful reading and helpful feedback on the manuscript, Davy Gérard and Frédéric Laux for providing elaborative information on results reported in Ref.¹⁴.

This work was supported by the RF Ministry of Education and Science, the State contract with Siberian Federal University for scientific research in 2017–2019. Numerical calculations were performed using the MVS-1000M system at the Institute of Computational Modeling of the Siberian Branch of the Russian Academy of Sciences.

- ¹S. Zou, N. Janel, and G. C. Schatz, *J. Chem. Phys.* **120**, 10871 (2004).
- ²S. Zou and G. C. Schatz, *J. Chem. Phys.* **121**, 12606 (2004).
- ³V. A. Markel, *J. Phys. B At. Mol. Opt. Phys.* **38**, L115 (2005).
- ⁴B. Auguie and W. L. Barnes, *Phys. Rev. Lett.* **101**, 143902 (2008).
- ⁵V. G. Kravets, F. Schedin, and A. N. Grigorenko, *Phys. Rev. Lett.* **101**, 1 (2008).
- ⁶Y. Chu, E. Schonbrun, T. Yang, and K. B. Crozier, *Appl. Phys. Lett.* **93**, 2006 (2008).
- ⁷R. Adato, A. A. Yanik, J. J. Amsden, D. L. Kaplan, F. G. Omenetto, M. K. Hong, S. Erramilli, and H. Altug, *Proc. Natl. Acad. Sci.* **106**, 19227 (2009).
- ⁸Z. Li, S. Butun, and K. Aydin, *ACS Nano* **8**, 8242 (2014).
- ⁹B. D. Thackray, V. G. Kravets, F. Schedin, G. Auton, P. A. Thomas, and A. N. Grigorenko, *ACS Photonics* **1**, 1116 (2014).
- ¹⁰R. R. Gutha, S. M. Sadeghi, and W. J. Wing, *Appl. Phys. Lett.* **110**, 153103 (2017).
- ¹¹W. Zhou, M. Dridi, J. Y. Suh, C. H. Kim, D. T. Co, M. R. Wasielewski, G. C. Schatz, and T. W. Odom, *Nat. Nanotechnol.* **8**, 506 (2013).
- ¹²G. Vecchi, V. Giannini, and J. Gómez Rivas, *Phys. Rev. Lett.* **102**, 146807 (2009).
- ¹³F. Laux, N. Bonod, and D. Gérard, *J. Phys. Chem. C* **121**, 13280 (2017).
- ¹⁴D. Khlopin, F. Laux, W. P. Wardley, J. Martin, G. A. Wurtz, J. Plain, N. Bonod, A. V. Zayats, W. Dickson, and D. Gérard, *J. Opt. Soc. Am. B* **34**, 691 (2017).
- ¹⁵Z.-S. Zhang, Z.-J. Yang, J.-B. Li, Z.-H. Hao, and Q.-Q. Wang, *Appl. Phys. Lett.* **98**, 173111 (2011).
- ¹⁶L. Lin and Y. Yi, *Opt. Express* **23**, 130 (2015).
- ¹⁷A. D. Humphrey, N. Meinzer, T. A. Starkey, and W. L. Barnes, *ACS Photonics* **3**, 634 (2016).
- ¹⁸N. Mahi, G. Lévêque, O. Saison, J. Marae-Djouda, R. Caputo, A. Gontier, T. Maurer, P.-M. Adam, B. Bouhafs, and A. Akjouj, *J. Phys. Chem. C* **121**, 2388 (2017).
- ¹⁹T. V. Teperik and A. Degiron, *Phys. Rev. B* **86**, 245425 (2012).
- ²⁰L.-H. Du, J. Li, Q. Liu, J.-H. Zhao, and L.-G. Zhu, *Opt. Mater. Express* **7**, 1335 (2017).
- ²¹M. Hentschel, M. Saliba, R. Vogelgesang, H. Giessen, A. P. Alivisatos, and N. Liu, *Nano Lett.* **10**, 2721 (2010).
- ²²V. Grigoriev, S. Varault, G. Boudarham, B. Stout, J. Wenger, and N. Bonod, *Phys. Rev. A* **88**, 063805 (2013).
- ²³D. Wang, A. Yang, A. J. Hryn, G. C. Schatz, and T. W. Odom, *ACS Photonics* **2**, 1789 (2015).
- ²⁴R. Nicolas, G. Lévêque, J. Marae-Djouda, G. Montay, Y. Madi, J. Plain, Z. Herro, M. Kazan, P.-M. Adam, and T. Maurer, *Sci. Rep.* **5**, 14419 (2015).
- ²⁵R. Guo, T. K. Hakala, and P. Törmä, *Phys. Rev. B* **95**, 155423 (2017).
- ²⁶N. Kinsey, M. Ferrera, V. M. Shalaev, and A. Boltasseva, *J. Opt. Soc. Am. B* **32**, 121 (2015).
- ²⁷B. D. Thackray, P. A. Thomas, G. H. Auton, F. J. Rodriguez, O. P. Marshall, V. G. Kravets, and A. N. Grigorenko, *Nano Lett.* **15**, 3519 (2015).
- ²⁸P. A. Thomas, G. H. Auton, D. Kundys, A. N. Grigorenko, and V. G. Kravets, *Sci. Rep.* **7**, 45196 (2017).
- ²⁹G. V. Naik, V. M. Shalaev, and A. Boltasseva, *Adv. Mater.* **25**, 3264 (2013).
- ³⁰U. Guler, V. M. Shalaev, and A. Boltasseva, *Mater. Today* **18**, 227 (2015).

- ³¹A. Lalis, G. Tessier, J. Plain, and G. Baffou, *J. Phys. Chem. C* **119**, 25518 (2015).
- ³²A. Catellani and A. Calzolari, *Phys. Rev. B* **95**, 115145 (2017).
- ³³L. Gui, S. Bagheri, N. Strohfeldt, M. Hentschel, C. M. Zgrabik, B. Metzger, H. Linnenbank, E. L. Hu, and H. Giessen, *Nano Lett.* **16**, 5708 (2016).
- ³⁴W. He, K. Ai, C. Jiang, Y. Li, X. Song, and L. Lu, *Biomaterials* **132**, 37 (2017).
- ³⁵R. Kamakura, S. Murai, S. Ishii, T. Nagao, K. Fujita, and K. Tanaka, *ACS Photonics* **4**, 815 (2017).
- ³⁶S. Bagheri, C. M. Zgrabik, T. Gissibl, A. Tittl, F. Sterl, R. Walter, S. De Zuani, A. Berrier, T. Stauden, G. Richter, E. L. Hu, and H. Giessen, *Opt. Mater. Express* **5**, 2625 (2015).
- ³⁷J. A. Briggs, G. V. Naik, T. A. Petach, B. K. Baum, D. Goldhaber-Gordon, and J. A. Dionne, *Appl. Phys. Lett.* **108**, 051110 (2016).
- ³⁸U. Guler, J. C. Ndukaife, G. V. Naik, A. G. A. Nnanna, A. V. Kildishev, V. M. Shalaev, and A. Boltasseva, *Nano Lett.* **13**, 6078 (2013).
- ³⁹J. A. Briggs, G. V. Naik, Y. Zhao, T. A. Petach, K. Sahasrabudhe, D. Goldhaber-Gordon, N. A. Melosh, and J. A. Dionne, *Appl. Phys. Lett.* **110**, 101901 (2017).
- ⁴⁰Y. Wang, A. Capretti, and L. Dal Negro, *Opt. Mater. Express* **5**, 2415 (2015).
- ⁴¹A. Perry and J. Schoenes, *Vacuum* **36**, 149 (1986).
- ⁴²H. Reddy, U. Guler, Z. Kudyshev, A. V. Kildishev, V. M. Shalaev, and A. Boltasseva, *ACS Photonics* **4**, 1413 (2017).
- ⁴³E. D. Palik, *Handbook of optical constants of solids II* (Academic Press, New York, 1998) p. 1096.
- ⁴⁴“Lumerical Solutions, FDTD Solutions,” .
- ⁴⁵N. Bonod and J. Neauport, *Adv. Opt. Photonics* **8**, 156 (2016).
- ⁴⁶B. Auguie, X. M. Bendaña, W. L. Barnes, and F. J. García de Abajo, *Phys. Rev. B* **82**, 155447 (2010).
- ⁴⁷A. G. Nikitin, T. Nguyen, and H. Dallaporta, *Appl. Phys. Lett.* **102**, 221116 (2013).
- ⁴⁸A. Vitrey, L. Aigouy, P. Prieto, J. M. García-Martín, and M. U. González, *Nano Lett.* **14**, 2079 (2014).
- ⁴⁹A. Abass, S. R.-K. Rodriguez, J. Gómez Rivas, and B. Maes, *ACS Photonics* **1**, 61 (2014).
- ⁵⁰A. I. Väkeväinen, R. J. Moerland, H. T. Rekola, A.-P. Eskelinen, J.-P. Martikainen, D.-H. Kim, and P. Törmä, *Nano Lett.* **14**, 1721 (2014).
- ⁵¹H. Reddy, U. Guler, A. V. Kildishev, A. Boltasseva, and V. M. Shalaev, *Opt. Mater. Express* **6**, 2776 (2016).
- ⁵²V. S. Gerasimov, A. E. Ershov, S. V. Karpov, A. P. Gavriluk, V. I. Zakomirnyi, I. L. Rasskazov, H. Ågren, and S. P. Polyutov, *Opt. Mater. Express* **7**, 555 (2017).
- ⁵³S.-Q. Li, W. Zhou, D. Bruce Buchholz, J. B. Ketterson, L. E. Ocola, K. Sakoda, and R. P. H. Chang, *Appl. Phys. Lett.* **104**, 231101 (2014).
- ⁵⁴J.-N. Liu, M. V. Schulmerich, R. Bhargava, and B. T. Cunningham, *Opt. Express* **22**, 18142 (2014).